

# Pairing and condensation in a resonant Bose-Fermi mixture

Elisa Fratini and Pierbiagio Pieri

*Dipartimento di Fisica, Scuola di Scienze e Tecnologie,  
Università di Camerino, Via Madonna delle Carceri 9, I-62032 Camerino, Italy*

(Dated: March 22, 2022)

We study by diagrammatic means a Bose-Fermi mixture, with boson-fermion coupling tuned by a Fano-Feshbach resonance. For increasing coupling, the growing boson-fermion pairing correlations progressively reduce the boson condensation temperature and make it eventually vanish at a critical coupling. Such quantum critical point depends very weakly on the population imbalance and for vanishing boson densities coincides with that found for the polaron-molecule transition in a strongly imbalanced Fermi gas, thus bridging two quite distinct physical systems.

PACS numbers: 03.75.Ss,03.75.Hh,32.30.Bv,74.20.-z

One of the main reasons behind the recent great interest in ultracold gases, is the possibility to reproduce physical systems relevant to other areas in physics, with a flexibility and a degree of tunability of physical parameters which is unimaginable in the original system of interest. The very same flexibility can also be used, however, to construct novel physical systems. A noticeable example of such novel systems, namely, resonant Bose-Fermi mixtures, will be here at issue. We will be interested in particular in the competition between boson-fermion pairing correlations and bosonic condensation, occurring in a mixture of single-component bosons and fermions when the boson-fermion pairing is made progressively stronger by means of a Fano-Feshbach resonance.

Initial theoretical studies of ultracold Bose-Fermi mixtures considered mainly non-resonant systems [1–5], where boson-fermion pairing is irrelevant, and studied, within mean-field like treatments, the tendency towards collapse or phase separation (as motivated by the first experimental results on non-resonant Bose-Fermi mixtures [6]). Bose-Fermi mixtures in the presence of a Fano-Feshbach resonance have been subsequently considered in [7–17], mostly for *narrow* resonances [7, 10–13, 16] and/or in specific contexts such as optical lattices, reduced dimensionality, zero temperature or vanishing density of one component [8, 9, 14, 15, 17].

Most of current experiments on Bose-Fermi mixtures [19–23] appear however to be closer to the case of a *broad* resonance, which is characterized by the smallness of the effective range parameter  $r_0$  of the interaction potential with respect to both the average interparticle distance and the scattering length [18]. Under these conditions, the resonant Bose-Fermi mixture is accurately described by a *minimal* Hamiltonian, made just by bosons and fermions mutually interacting via an attractive point-contact potential. This Hamiltonian is simpler and more “fundamental” in character than its counterpart for a narrow resonance because of the absence of any other parameter besides the strength of the boson-fermion interaction. In addition, its simplicity allows the implementation of more sophisticated many-

body calculations (beyond mean-field).

We thus consider the following (grand-canonical) Hamiltonian:

$$H = \sum_s \int d\mathbf{r} \psi_s^\dagger(\mathbf{r}) \left( -\frac{\nabla^2}{2m_s} - \mu_s \right) \psi_s(\mathbf{r}) + v_0 \int d\mathbf{r} \psi_B^\dagger(\mathbf{r}) \psi_F^\dagger(\mathbf{r}) \psi_F(\mathbf{r}) \psi_B(\mathbf{r}) \quad (1)$$

Here  $\psi_s^\dagger(\mathbf{r})$ , creates a particle of mass  $m_s$  and chemical potential  $\mu_s$  at spatial position  $\mathbf{r}$ , where  $s = B, F$  indicates the boson and fermion atomic species, respectively, while  $v_0$  is the bare strength of the contact interaction (we set  $\hbar = k_B = 1$  throughout this paper). Ultraviolet divergences associated with the use of a contact interaction in (1) are eliminated, as for two-component Fermi gases [24], by expressing the bare interaction  $v_0$  in terms of the boson-fermion scattering length  $a$  via the (divergent) expression  $1/v_0 = m_r/(2\pi a) - \int 2m_r/\mathbf{k}^2 d\mathbf{k}/(2\pi)^3$ , where  $m_r = m_B m_F/(m_B + m_F)$  is the reduced mass.

The Hamiltonian (1) does not contain explicitly the boson-boson interaction. Provided it is repulsive and non-resonant, this interaction yields in fact a mean-field shift, which consists in a simple redefinition of the boson chemical potential (attractive boson-boson interactions would lead to mechanical instability and are excluded from our consideration). S-wave interaction between fermions is finally excluded by Pauli principle.

The effective coupling strength in the many-body system is determined by comparing the boson-fermion scattering length  $a$  with the average interparticle distance  $n^{-1/3}$  (with  $n = n_B + n_F$ , where  $n_B$  and  $n_F$  are the boson and fermion particle number density, respectively). In particular, we will use the same dimensionless coupling strength  $(k_F a)^{-1}$  normally used for two-component Fermi gases, where the wave-vector  $k_F \equiv (3\pi^2 n)^{1/3}$  (note that  $k_F$  coincides with the noninteracting Fermi wave-vector  $k_F^0 = (6\pi^2 n_F)^{1/3}$  only for  $n_B = n_F$ ).

The expected behavior of the system is clear in the two opposite limits of the boson-fermion coupling. In the weak-coupling limit, where the scattering length  $a$  is small and negative (such that  $(k_F a)^{-1} \ll -1$ ), the

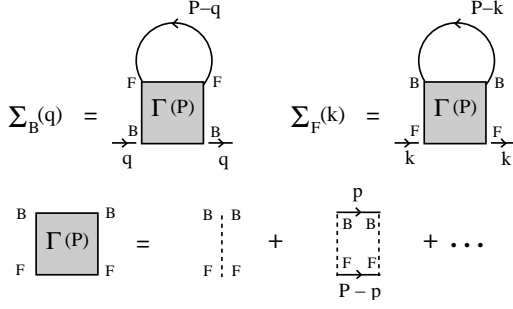


FIG. 1: T-matrix diagrams for the fermionic and bosonic self-energies in the normal phase. Full lines represent bare bosonic (BB) and fermionic (FF) Green's functions. Broken lines represent bare boson-fermion interactions  $v_0$ .

two components will behave essentially as ideal Bose and Fermi gases. Bosons will condense at  $T_c = 3.31n_B^{2/3}/m_B$ , while fermions will fill out (at sufficiently low temperature) a Fermi sphere with radius  $k_F^0$ , the chemical potentials  $\mu_B$  and  $\mu_F$  being modified with respect to their noninteracting values by the mean-field shifts  $2\pi n_F a/m_r$ , and  $2\pi n_B a/m_r$ , respectively. In the opposite strong-coupling limit where  $a$  is small and positive (such that  $(k_F a)^{-1} \gg 1$ ), bosons will pair with fermions to form tightly bound fermionic molecules, with binding energy  $\epsilon_0 = 1/(2m_r a^2)$ . In particular, in systems where  $n_B \leq n_F$ , on which we focus in the present paper, all bosons will eventually pair with fermions into molecules, suppressing condensation completely.

In a complete analogy with the BCS-BEC crossover problem in a two-component Fermi gas [24], the choice of the self-energy diagrams will be guided by the criterion that a single set of diagrams should recover the correct physical description of the two above opposite limits. In the *normal* phase above the condensation critical temperature  $T_c$ , to which we restrict in the present paper, this condition is met (as we shall see below) by the T-matrix choice of diagrams represented in Fig. 1, yielding the expressions:

$$\Sigma_B(q) = -\frac{1}{\beta} \int \frac{d\mathbf{P}}{(2\pi)^3} \sum_m G_F^0(P-q) \Gamma(P) \quad (2)$$

$$\Sigma_F(k) = \frac{1}{\beta} \int \frac{d\mathbf{P}}{(2\pi)^3} \sum_m G_B^0(P-k) \Gamma(P) \quad (3)$$

for the bosonic and fermionic self-energies  $\Sigma_B$  and  $\Sigma_F$ , where  $G_B^0$  and  $G_F^0$  are bare bosonic and fermionic Green's functions and  $\Gamma(P)$  is the many-body T-matrix:

$$\Gamma(P) = -\left\{ \frac{m_r}{2\pi a} + \int \frac{d\mathbf{p}}{(2\pi)^3} \times \left[ \frac{1 - f[\xi_F(\mathbf{P}-\mathbf{p})] + b[\xi_B(\mathbf{p})]}{\xi_F(\mathbf{P}-\mathbf{p}) + \xi_B(\mathbf{p}) - i\Omega_m} - \frac{2m_r}{\mathbf{p}^2} \right] \right\}^{-1} \quad (4)$$

In the above expressions  $q = (\mathbf{q}, \omega_\nu)$ ,  $k = (\mathbf{k}, \omega_n)$ ,

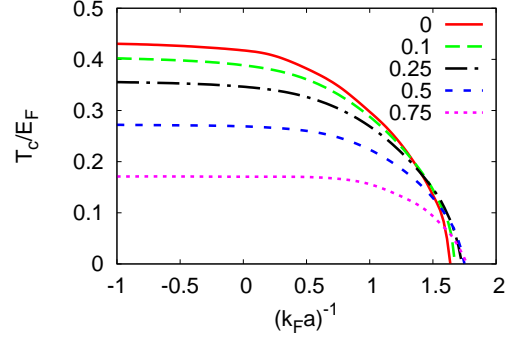


FIG. 2: Critical temperature (in units of  $E_F = k_F^2/2m_F$ ) for condensation of bosons vs the boson-fermion coupling  $(k_F a)^{-1}$  for different values of the density imbalance  $(n_F - n_B)/n$  in a mixture with  $m_B = m_F$ .

$P = (\mathbf{P}, \Omega_m)$ , where  $\omega_\nu = 2\pi\nu/\beta$  and  $\omega_n = (2n+1)\pi/\beta$ ,  $\Omega_m = (2m+1)\pi/\beta$  are bosonic and fermionic Matsubara frequencies, respectively ( $\beta = 1/T$  being the inverse temperature and  $\nu, n, m$  integer), while  $f(x)$  and  $b(x)$  are the Fermi and Bose distribution functions and  $\xi_s(\mathbf{p}) = \mathbf{p}^2/(2m_s) - \mu_s$ . The above self-energies determine finally the dressed Green's functions  $G_s^{-1} = G_s^0^{-1} - \Sigma_s$  entering the particle numbers equations:

$$n_B = -\int \frac{d\mathbf{q}}{(2\pi)^3} \frac{1}{\beta} \sum_\nu G_B(\mathbf{q}, \omega_\nu) e^{i\omega_\nu 0^+} \quad (5)$$

$$n_F = \int \frac{d\mathbf{k}}{(2\pi)^3} \frac{1}{\beta} \sum_n G_F(\mathbf{k}, \omega_n) e^{i\omega_n 0^+}. \quad (6)$$

Equations (2–6) fully determine the thermodynamic properties of the Bose-Fermi mixture in the normal phase. This phase is characterized by the condition  $\mu_B - \Sigma_B(q=0) < 0$ ; upon lowering the temperature, condensation will then occur when  $\mu_B = \Sigma_B(q=0)$ .

Analytic results can be obtained in the two opposite limits of the boson-fermion coupling [25]. For weak-coupling  $\Gamma(P) \simeq -\frac{2\pi a}{m_r}$ , yielding  $\Sigma_B \simeq 2\pi n_F a/m_r$  and  $\Sigma_F \simeq 2\pi n_B a/m_r$ , in accordance with the expected mean-field shifts. For strong-coupling  $\Gamma(P)$  gets instead proportional to the molecular propagator:

$$\Gamma(P) \simeq -\frac{2\pi}{m_r^2 a} \frac{1}{i\Omega_m - \frac{\mathbf{P}^2}{2M} + \mu_M} \quad (7)$$

where  $\mu_M \equiv \mu_B + \mu_F + \epsilon_0$  is the molecular chemical potential and  $M = m_B + m_F$ . Insertion of this propagator in Eqs. (2–6) leads, for  $n_B < n_F$ , to  $\mu_M \simeq (6\pi^2 n_B)^{2/3}/2M$ ,  $\mu_F \simeq [6\pi^2(n_F - n_B)]^{2/3}/2m_F$  and  $\mu_B = \mu_M - \mu_F - \epsilon_0 \simeq -\epsilon_0$ , as expected when all bosons pair with fermions.

For intermediate values of the boson-fermion coupling Eqs. (2–6) need to be solved numerically. The results for the condensation critical temperature  $T_c$  vs the boson-fermion dimensionless coupling  $(k_F a)^{-1}$  are presented in

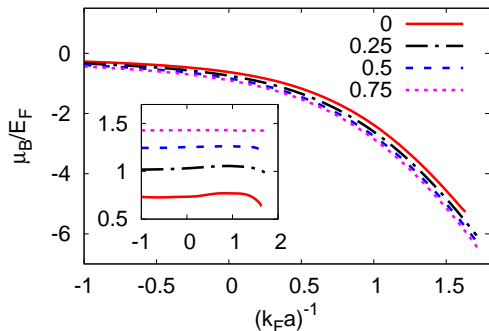


FIG. 3: Boson chemical potential at the critical temperature  $T_c$  (in units of  $E_F$ ) vs the boson-fermion coupling  $(k_F a)^{-1}$  for different values of the density imbalance  $(n_F - n_B)/n$  in a mixture with  $m_B = m_F$ . The corresponding fermion chemical potential is reported in the inset.

Fig. 2 for a mixture with  $m_B = m_F$  at several values of density imbalance. [26] All curves start in weak-coupling from the corresponding noninteracting values, and decrease monotonically for increasing coupling due to the growing pairing correlations, which tend to deplete the zero momentum mode and distribute the bosons over a vast momentum region, as required to build the internal molecular wave-function. The critical temperature vanishes eventually at a critical coupling, corresponding to a quantum critical point which separates a phase with a condensate from a phase where molecular correlations are so strong to deplete the condensate completely.

Remarkably, the critical coupling value depends very weakly on the degree of density imbalance: all curves terminate in the narrow region  $1.6 < (k_F a)^{-1} < 1.8$ . In this respect, it is interesting to consider the limit  $n_B \rightarrow 0$ , where the critical coupling can be calculated independently by solving the problem of a single boson immersed in a Fermi sea. This is actually the same as a spin-down fermion immersed in a Fermi sea of spin-up fermions, since for a single particle the type of statistics is immaterial. The critical coupling reduces then to that for the polaron-to-molecule transition, recently studied in the context of strongly imbalanced *two-component Fermi gases* [27–33]. In particular, the solution of our equations in this limit yields the critical coupling  $(k_F a)^{-1} = 1.60$ , in full agreement with the value  $(k_F^\uparrow a)^{-1} = 1.27$  (where  $k_F^\uparrow = 2^{1/3} k_F$ ) reported in [32, 33] for the polaron-to-molecule transition, when treated at the same level of approximation [34, 36]. The meeting of the properties of a Bose-Fermi mixture with those of a two-component Fermi mixture at this point of the phase diagram is quite remarkable, especially because, according to our results of Fig. 1, this “universal” point sets the scale for the quantum phase transition for *all* boson densities  $n_B \leq n_F$ .

The chemical potentials  $\mu_B$  and  $\mu_F$  at  $T_c$  vs.  $(k_F a)^{-1}$

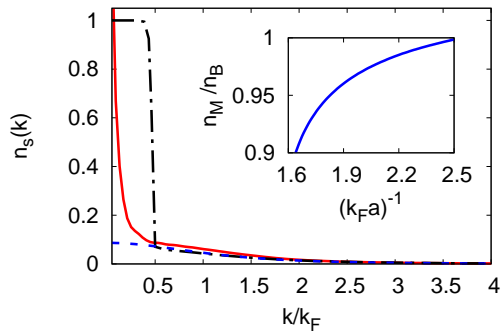


FIG. 4: Boson (full line) and fermion (dashed-dotted) momenta distribution curves for  $n_B = n_F$ ,  $m_B = m_F$ ,  $(k_F a)^{-1} = 1.63$  and  $T = T_c \simeq 0.015 E_F$ . See text for the meaning of the dashed curve. The inset reports the fraction of molecules vs  $(k_F a)^{-1}$  for the same mixture at  $T = 0.1 E_F$ .

are reported in Fig. 3, for different values of the density imbalance. The two chemical potentials behave quite differently. The fermion chemical potential remains almost constant in the whole range of coupling considered; the boson chemical potential, on the other hand, diminishes quite rapidly with increasing coupling while depending little on the density imbalance. This different behavior results from the concurrence of several factors. For weak-coupling, the increasing (negative) mean-field shift of the fermion chemical potential for increasing coupling is partially compensated by the decrease of the temperature when moving along the critical line. On the molecular side, the fermion chemical potential is instead determined by the Fermi energy of the unpaired fermions plus a mean-field shift caused by interaction with molecules. Pauli repulsion makes this interaction repulsive [8, 25] thus keeping the fermion chemical potential positive. The boson chemical potential, on the other hand, interpolates between the mean-field value  $2\pi n_F a / m_r$  in weak coupling and  $\mu_B \approx -\epsilon_0$  in strong coupling, as required by molecule formation.

Figure 4 reports the momentum distributions  $n_B(\mathbf{k})$  and  $n_F(\mathbf{k})$  (as obtained before momentum integration in Eqs. (5)-(6)) at  $T_c$ , for a mixture with  $n_B = n_F$ , at the coupling value  $(k_F a)^{-1} = 1.63$  (approximately at the quantum critical point). The two distributions are markedly different at low momenta, consistently with their different statistics, but coalesce into the same behavior just after the step in the fermion momentum distribution. This common behavior corresponds to the function  $n_M |\phi(\mathbf{k})|^2$  (dashed line in Fig. 4), where  $\phi(\mathbf{k}) = (8\pi a^3)^{1/2} / (\mathbf{k}^2 a^2 + 1)$  is the normalized two-body internal wave function of the molecules, while the coefficient  $n_M$  represents their density. In the present case  $n_M = 0.89 n_B$ , showing that a fraction of bosons remains unpaired but still does not condense even at such

a low temperature. The extrapolation of these results at exactly zero temperature indicates the existence (in a coupling range starting right after the quantum critical point) of quite an unconventional Bose liquid, corresponding to the unpaired bosons, which do not condense even at zero temperature. The fraction of unpaired fermions is instead more conventional and consists in a Fermi liquid, which is responsible for the jump in the fermion momentum distribution. In particular, the position of the jump in Fig. 4 at  $|\mathbf{k}| \simeq 0.47 k_F$ , corresponds to an “enclosed” density of  $0.10 n_F$ , in good numerical agreement with the value  $0.11 n_F$  obtained from the Luttinger theorem [37] for the fraction  $(n_F - n_M)$  of unpaired fermions (using the value  $n_M = 0.89 n_B$  extracted independently above). Note finally that the number of unpaired bosons progressively decreases by increasing the coupling, as expected on physical grounds, reaching eventually a 100% conversion of bosons into molecules, as shown in the inset of Fig. 4, where the ratio  $n_M/n_B$  is reported vs coupling at a constant temperature.

We wish to conclude finally by commenting on three-body losses and mechanical instabilities, that could prevent the experimental observation of the many-body physics described above. The choice of restricting our analysis to mixtures with a majority of fermions was precisely aimed at reducing the importance of these nuisances. Three-body losses are dominated by processes involving two bosons and one fermion, with a rate proportional to  $n_B^2 n_F$  [22]. They can thus be controlled by keeping  $n_B$  sufficiently small with respect to  $n_F$ . A predominance of fermions should also reduce the tendency to collapse, because of the stabilizing effect of Fermi pressure. As a matter of fact, we have verified that the compressibility matrix  $\partial\mu_s/\partial n_{s'}$  remained positive definite for all couplings, temperatures, and densities  $n_F \geq n_B$  considered in our calculations. Apparently, pairing correlations act to protect the system from the mean field instabilities dominating the phase diagram of non-resonant Bose-Fermi mixtures. Resonant Bose-Fermi mixtures with a majority of fermions appear thus promising systems for the observation of a rich many-body physics.

We thank F. Palestini, A. Perali, and G.C. Strinati for a careful reading of the manuscript. Partial support by the Italian MIUR under Contract Cofin-2007 “Ultracold atoms and novel quantum phases” is acknowledged.

---

[1] L. Viverit, C.J. Pethick, and H. Smith, Phys. Rev. A **61**, 053605 (2000).  
 [2] X.X. Yi and C.P. Sun, Phys. Rev. A **64**, 043608 (2001).  
 [3] A. Albus *et al.*, Phys. Rev. A **65**, 053607 (2002).  
 [4] R. Roth and H. Feldmeier, Phys. Rev. A **65**, 021603(R) (2002).  
 [5] M. Lewenstein *et al.*, Phys. Rev. Lett. **92**, 050401 (2004).  
 [6] G. Modugno *et al.*, Science **297**, 2240 (2002).

[7] L. Radzihovsky, J. Park, and P.B. Weichman, Phys. Rev. Lett. **92**, 160402 (2004).  
 [8] M.Y. Kagan *et al.*, Phys. Rev. A **70**, 023607 (2004).  
 [9] A. Storozhenko *et al.*, Phys. Rev. A **71**, 063617 (2005).  
 [10] D.B.M. Dickerscheid, *et al.*, Phys. Rev. Lett. **94**, 230404 (2005).  
 [11] S. Powell, S. Sachdev, and H.P. Buchler, Phys. Rev. B **72**, 024534 (2005).  
 [12] A.V. Avdeenkov, D.C.E. Bortolotti, and J.L. Bohn, Phys. Rev. A **74**, 012709 (2006).  
 [13] L. Pollet *et al.*, Phys. Rev. A **77**, 023608 (2008).  
 [14] M. Rizzi and A. Imambekov, Phys. Rev. A **77**, 023621 (2008).  
 [15] T. Watanabe, T. Suzuki, and P. Schuck, Phys. Rev. A **78**, 033601 (2008).  
 [16] F.M. Marchetti *et al.*, Phys. Rev. B **78**, 134517 (2008).  
 [17] I. Titvinidze, M. Snoek, and W. Hofstetter, Phys. Rev. B **79**, 144506 (2009).  
 [18] S. Simonucci, P. Pieri, and G.C. Strinati, Europhys. Lett. **69**, 713 (2005).  
 [19] K. Günter *et al.*, Phys. Rev. Lett. **96**, 180402 (2006).  
 [20] C. Ospelkaus *et al.*, Phys. Rev. Lett. **97**, 120402 (2006).  
 [21] S. Ospelkaus *et al.*, Phys. Rev. Lett. **97**, 120403 (2006).  
 [22] J.J. Zirbel *et al.*, Phys. Rev. Lett. **100**, 143201 (2008).  
 [23] K.-K. Ni *et al.*, Science **322**, 231 (2008).  
 [24] P. Pieri and G.C. Strinati, Phys. Rev. B **61**, 15370 (2000).  
 [25] Details of the analytic calculations will be presented elsewhere (E. Fratini and P. Pieri, in preparation).  
 [26] Numerical calculations will be limited to the case  $m_B = m_F$  to restrict the space parameter. This case is directly applicable to isotopic mixtures of sufficiently heavy atoms ( $^{39}\text{K}$ - $^{40}\text{K}$ , e.g.), but it is taken as representative of the more general situation.  
 [27] A. Schirotzek *et al.*, Phys. Rev. Lett. **102**, 230402 (2009).  
 [28] M. Veillette *et al.*, Phys. Rev. A **78**, 033614 (2008).  
 [29] N.V. Prokof'ev and B.V. Svistunov, Phys. Rev. B **77**, 125101 (2008).  
 [30] P. Massignan, G.M. Bruun, and H.T.C. Stoof, Phys. Rev. A **78**, 031602(R) (2008).  
 [31] C. Mora and F. Chevy, Phys. Rev. A **80**, 033607 (2009).  
 [32] M. Punk, P.T. Dumitrescu, and W. Zwerger, Phys. Rev. A **80**, 053605 (2009).  
 [33] R. Combescot, S. Giraud, and X. Leyronas, arXiv:0907.3197 (2009).  
 [34] QMC calculations [29] and refined diagrammatic approximations [33] for the single spin-down problem yield the value  $(k_F a)^{-1} = 1.11$  for the polaron-to-molecule transition, a 30% off the T-matrix prediction. This difference is due to the overestimate of the molecule-fermion repulsion by the T-matrix approximation, which yields  $8/3a$  for the molecule-fermion scattering length in place of the exact value  $1.18a$  [35], thus making the molecule formation in a Fermi sea environment less convenient.  
 [35] G.V. Skorniakov and K.A. Ter-Martirosian, Zh. Eksp. Teor. Fiz. **31**, 775 (1956) [Sov. Phys. JETP **4**, 648 (1957)].  
 [36] The value 1.60 for the critical coupling in the limit  $n_B \rightarrow 0$  is reached with a weak reentrant behavior of the critical coupling vs. imbalance, occurring at imbalances larger than those reported in Fig. 1. For instance, at imbalance 0.95,  $T_c$  vanishes at  $(k_F a)^{-1} \simeq 1.63$ .  
 [37] J.M. Luttinger, Phys. Rev. **116**, 1153 (1960).